Biosensors and Bioelectronics 142 (2019) 111533

Contents lists available at ScienceDirect

Biosensors and Bioelectronics

journal homepage: www.elsevier.com/locate/bios

The strategy of antibody-free biomarker analysis by in-situ synthesized molecularly imprinted polymers on movable valve paper-based device

Ji Qi[a,b,1], Bowei Li[b,**,1], Na Zhou[b], Xiaoyan Wang[b,c], Dongmei Deng[a], Liqiang Luo[a,***], Lingxin Chen[b,*]

[a] College of Sciences, Shanghai University, Shanghai 200444, China
[b] CAS Key Laboratory of Coastal Environmental Processes and Ecological Remediation; Research Center for Coastal Environmental Engineering and Technology, Yantai Institute of Coastal Zone Research, Chinese Academy of Sciences, Yantai 264003, China
[c] School of Pharmacy, Binzhou Medical University Yantai 264003, China

ARTICLE INFO

Keywords:
Paper based microfluidic device
Bioinspired molecularly imprinted technique
Electrochemical detection
Valve
Point of care diagnosis
Cancer markers

ABSTRACT

In this work, we provided a novel strategy of antibody-free biomarker analysis by in-situ synthesized molecularly imprinted polymers (MIPs) on movable valve microfluidic paper-based electrochemical device (Bio-MIP-ePADs) for clinical detection of biomarkers. The newly movable valves on the device enable continuous and convenient delivery of fluid, which guarantee the performance for fabricating MIPs structure during long time electropolymerization. Moreover, this strategy can directly detect antigens by taking advantage of molecular imprinting on paper-based device, which greatly decreases the cost during clinical testing, reduces the tedious washing procedure and does not need to consider the preservation of the antibody in enzyme linked immunosorbent assay (ELISA). This feature makes the chip suitable for the on-site family treatment or commercial products. To further validate the applicability of this proposed method for clinical diagnostic testing, carcinoembryonic antigen (CEA) was applied as prototyping model target for the clinical analysis. The proposed Bio-MIP-ePADs were cheap, easy to prepare, disposable and provided reliable analysis by comparing with ELISA. We hope the application of this technology will open up a new avenue to the point-of-care testing (POCT).

1. Introduction

Analysis of biomarkers in humans is an effective method of medical diagnosis (Jones, 2010). Along with the development of biological sciences, more and more biomarkers have been discovered and used for diagnosing human diseases (Huang and Vakoc, 2016; Liotta et al., 2003). Among them, the analysis of cancer markers is widely used in the diagnosis of tumor incidence, but the diagnosis of cancers often delays the optimal treatment opportunity due to lack of time. Therefore, it is important to provide the relative device for cancer marker analysis and with the characteristics including less sample requirement, inexpensive cost, and easy to use (Kumar et al., 2015; Yamada et al., 2017). In addition, the extensive variety of measurable cancer biomarkers, greater sensitivity, higher informative and low-cost analytical techniques improve diagnostic reliability (Gervais et al., 2011). Enzyme linked immunosorbent assay (ELISA) is a popular clinical and laboratory technique that is widely used for cancer biomarkers analysis. However, it suffers some limitations such as high cost of antibodies, strict preservation conditions, long reaction time and tedious washing procedure (Cheng et al., 2010).

In some ways, the molecular imprinted polymer appears to be a better option that compared to the biological antibodies (Gui et al., 2018). Molecular imprinted polymers (MIPs) have attracted much attention due to unique properties, such as simplicity, low cost, facile preparation, storable, high selectivity and sensitivity (Cai et al., 2010; Chen et al., 2011; Qi et al., 2018; Wulff, 2002). MIPs-based electrochemical sensors have some great advantages such as high selectivity and sensitivity, chemical/mechanical stability, reusability, and low limit of detection (LOD) (Chen et al., 2016; Haupt and Mosbach, 2000; Yang et al., 2018). However, one of the remaining challenges is that the biological analytes are difficult to be buried in the interiors of the MIPs to form binding site. Herein, tlectropolymerization method is a suitable

* Corresponding author.
** Corresponding author.
*** Corresponding author.
E-mail addresses: bwli@yic.ac.cn (B. Li), luck@shu.edu.cn (L. Luo), lxchen@yic.ac.cn (L. Chen).
[1] These authors contributed equally: Ji Qi, Bowei Li.

https://doi.org/10.1016/j.bios.2019.111533
Received 22 May 2019; Received in revised form 12 July 2019; Accepted 22 July 2019
Available online 24 July 2019
0956-5663/

synthesis method of MIPs on μPADs, due to its many advantages, such as simple preparation procedures, easy control of the MIPs layer thickness, and uniform polymer distribution on the electrode surface (Chen et al., 2017; Lee et al., 2007; Liang et al., 2017; Liu et al., 2006; Xie et al., 2010; Yang et al., 2017).

The microfluidic paper-based device (μPADs) was firstly introduced as a diagnostic device in 2007 (Martinez et al., 2007). As a low-cost and user-friendly alternative to traditional laboratory testing, it is improved the accessibility of medical diagnostics under simple conditions (Gong and Sinton, 2017; Hu et al., 2014). Microfluidic paper-based chips have also opened up its diversified development in the field of analysis and diagnosis (Yetisen et al., 2013). The progress of electrochemical analysis on microfluidic chip platforms has enhanced the portability and practicality of electrochemical analysis devices (Economou et al., 2018). Dungchai et al. reported the first demonstration of electrochemical detection for paper-based microfluidic devices (Dungchai et al., 2009). Eric's group developed an electrochemical cell on a paper-based analytical device for the exhaustive determination of halides in a range of diverse water samples and food supplements (Cuartero et al., 2015). Ding et al. reported a three-dimensional origami paper-based device, in which a solid-contact ion-selective electrode was integrated with an all-solid-state reference electrode (Ding et al., 2016). Ruecha et al. developed a fully inkjet-printed disposable and low cost paper-based device for potentiometric Na^+ or K^+ ion sensing (Ruecha et al., 2017a). The evolution of paper-based platform was not only developed the process of chemical analysis, but it was also treated some necessary synthesis and reaction which need to be completed on paper chip (Boehle et al., 2018; Ge et al., 2017; Morbioli et al., 2017). Li et al. reported a novel flower-like Ag@Au hybrids modified microfluidic paper-based electrochemical device was prepared by a two-step growth approach and served as sensor platform for detection of CA-125 (Li et al., 2014). Sun et al. reported a novel rotational paper-based analytical device to implement multi-step electrochemiluminescence (ECL) immunoassays (Sun et al., 2018). The synthesis of advanced materials and the utilization of analytical methods have improved the practicality and reliability of analytical diagnostics under microfluidic paper-based device (Li et al., 2017b). Some advanced materials have tended to be synthesized in situ on the surface of paper fibers, such as gold nanoparticles (Choleva et al., 2015; Nunez-Bajo et al., 2018; Ruecha et al., 2017b), ZnO nanoparticles (Kong et al., 2018; Manekkathodi et al., 2010), carbon material (de Araujo et al., 2017) and polymers (Kjellgren et al., 2006; Wang et al., 2013). Yu et al. reported microfluidic paper-based analytical devices through electropolymerization of molecular imprinted polymer (MIP) in a novel Au nanoparticle (AuNP) modified paper working electrode (Au-PWE) for detection of D-glutamic acid (Ge et al., 2013). The fastness and uniformity of the modified materials are enhanced by direct synthesis on the μPADs. In addition, the process of grafting the materials is also simplified. Further, it has excellent prospects in simplifying synthesis process, reducing costs, and improving the performance of analysis (Mahadeva et al., 2015). However, as the complexity of the reaction system increases, more function needs to be completed on the μPADs in a reasonable manner (Wang et al., 2017; Zhang et al., 2018). It is hopeful that the movable valve can be served as a convenient and free way to transport fluid continuously to completed multi-step and long-term reaction on the paper-based microfluidic devices (Han et al., 2018; Li et al., 2017a).

In this paper, we designed a novel strategy to fabricate microfluidic paper-based analytical devices (μPADs) based on a surface bio-molecularly-imprinted technique for selective and sensitive clinical detection of carcino-embryonic antigen (CEA) through movable valve design and origami method. The movable valve's movement was realized using hollow rivets as the holding center to control channel of the ePADs in different layers, which improved the performance during the period of synthesis and detection significantly. Graphene oxide, chitosan and CEA templates were assembled on the μPADs as a substrate, and subsequently the molecularly imprinted layer were formed by electropolymerization of dopamine (DA). Because the entire manufacturing process was carried out on the μPADs without any external treatment, the proposed method has the characteristics of green synthesis, low cost, and low toxicity. It is worth noting that the design of the movable valve on such a paper-based microfluidic device enables continuous delivery of fluid, which is convenient and facile to carry out multi-step electropolymerization during a long time (~1 h). And the paper chip is disposable, lightweight and easy-to-use. To our best knowledge, this is the first time a paper-based MIP electrochemical sensor was presented that contained the bio-molecularly imprinted polymers has been successfully synthesized and applied for detection of cancer biomarkers by movable valve design on μPADs.

2. Experimental

2.1. Materials and instruments

Dopamine (DA), graphene oxide (GO), chitosan were provided by Sigma-Aldrich (USA). Carcino-embryonic antigen (CEA) was obtained from Linc-Bio Science Co., Ltd. (Shanghai, China). K_2HPO_4, KH_2PO_4, $K_3Fe(CN)_6$ and $K_4Fe(CN)_6{\cdot}3H_2O$ were bought from Sinopharm Chemical Reagent Co., Ltd. (China). Milli-Q water (18.25 MΩ cm) was used throughout the experiments. The clinical human serum samples were obtained from Xin Hua Hospital Affiliated to Shanghai Jiao Tong University School of Medicine and Binzhou Medical University Hospital. The Whatman No.1 chromatography filter paper was purchased from GE Company (Shanghai, China). Carbon ink and Silver/silver chloride ink (CNC-01) were purchased from Xuzhou Bohui New Materials Tech. Co. Ltd (Jiangsun, China). The hollow rivets, hammer and puncher were obtained from local stores. The paper-based chip was fabricated using a commercial solid-wax printer (XEROX Phaser 8560DN). Electrochemical measurements were performed on CHI 1030C electrochemical workstation (Shanghai CH Instrument Co., China). Electrochemical impedance spectroscopy (EIS) measurements were tested on a Solartron 1255B Frequency Response Analyzer/SI 1287 Electrochemical Interface (Scribner Associates, Inc., USA) using 5 mM $[Fe(CN)_6]^{3-/4-}$ as the electrochemical probe. Modifications of the paper were recorded by scanning electron microscopy (SEM; JSM 5600 LV). CEA ELISA kit was purchased from Biocell Biotechnol. Co., Ltd. (China). The optical density was measured on a microplate reader (TECAN Infinite 200 M PRO NanoQuant).

2.2. Design and assembly of ePADs

The progress of paper fabrication used the same way by our previous reports (Li et al., 2017b). Briefly, we use printer (XEROX Phaser 8560DN) for designing a structure that contains hydrophobic and hydrophilic areas on the paper chip. After 30 s of wax melting at 150 °C, the wax penetrated the paper creating a barrier that blocks the flow of water. The working electrode, counter electrode and reference electrode were manual brushed on the paper using carbon ink and silver/silver chloride ink, respectively (Ding et al., 2016). Each component of the chip was cut by a scissor and holes were punched on the chip before assembly.

Four parts of paper-based chips were designed to fabricate ePADs. They were the working electrode part, counter/reference electrode part, movable valve part and washing channels part that connected to the working electrode part, respectively. The counter/reference electrode part and the movable valve part were connected to the working electrode part by rivets. The washing channels part was connected and used by origami folding. On the working electrode part (50 mm × 25 mm), there were two circular sample pools (9 mm in diameter) that manual brushed with two carbon working electrodes on the opposite side respectively, a synthetic material pool (5 mm in diameter) and two channels (2 mm width) to the sample pools which were disconnected. The counter/reference electrode part (24 mm in

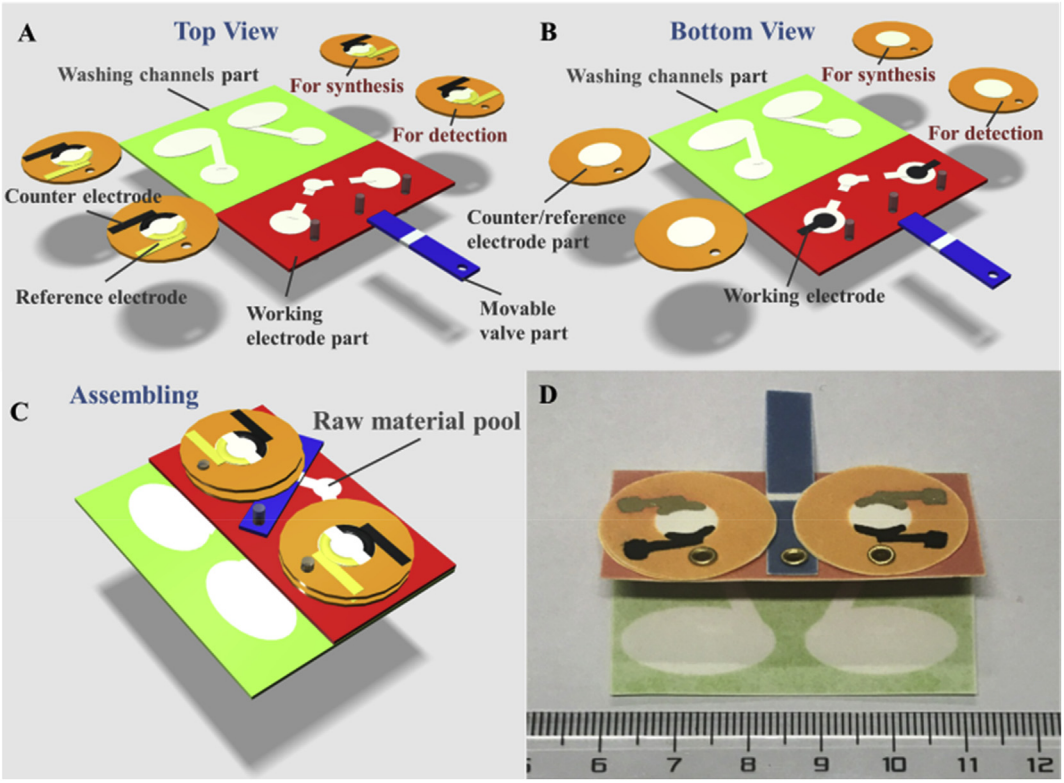

Fig. 1. Schematic diagram of Bio-MIP-ePADs. (A)Three-dimensional structural schematic of components of Bio-MIP-ePADs contained working electrode part (red color), four counter/reference electrode parts (yellow color), washing channels part (green color) and movable valve part (blue color) in top view. (B) The bottom view of three-dimensional structural schematic of components of Bio-MIP-ePADs. (C) Three-dimensional schematic of fully integrated Bio-MIP-ePADs. The synthetic material pool and sample pools could be connected by movable valve. (D) The photographs of the top view and size measurement of the constructed Bio-MIP-ePADs. (For interpretation of the references to colour in this figure legend, the reader is referred to the Web version of this article.)

diameter) contained carbon counter electrode and silver/silver chloride reference electrode on an unprinted hydrophilic area where same as working electrodes part. The unprinted hydrophilic area (sample pool) constituted the reservoir of the paper-based electrochemical cell after being overlapped with sample pool of working electrode part. The sample cell for each working electrode was equipped with two counter/reference electrode chips, one for synthesis process and the other for detection process. The washing channels part (40 mm × 50 mm) has hydrophobic channels and two waste pools for transporting waste solution.

2.3. Fabrication of bio-MIP-ePADs

The Bio-MIP-ePADs were prepared by surface imprinting technology as following. Firstly, all of the counter/reference electrode parts were rotated away from the working electrode part. 5.0 μL of GO was added to the sample pools of working electrode part and dried at room temperature. Then, 5.0 μL of 0.25 mg/mL chitosan was added to the sample pools of working electrode part and dried at room temperature. Subsequently, 5.0 μL of 2.5% glutaraldehyde was added and incubated for 2 h in room temperature (Sun et al., 2018). After completing the above steps, the washing channels part was folded for washing with washing buffer (PBS, 10 mM, pH = 7.4). Secondly, 5 μL of 50 μg/mL CEA was added to sample pools as template molecular. After 30 min equilibrium, one counter/reference electrode part was rotated to overlap with the sample pool of working electrode part to form an electrochemical cell and the movable valve was open. The paper chip was fixed and connected to the electrochemical workstation (Shanghai CH Instrument Co., China). A phosphate buffer solution (10 μL, 10 mM, pH = 7.4, 25 °C) containing dopamine (5 mM) were added into the synthetic material pool of working electrode part, and flowed through the hydrophobic channel to the sample cell. Thirty seconds later, the movable valve closed and dopamine starts to polymerize through 10 cycles of cyclic voltammetry (CVs) in a potential range between −0.5 V and 0.5 V at a scan rate of 20 mV/s and room temperature(Chen et al., 2017; Liu et al., 2006). After 10 cycles of scanning, the movable valve was moved open, and another phosphate buffer solution (10 μL, 10 mM, pH = 7.4, 25 °C) containing dopamine (10 mM) were added into the synthetic material pool of working electrode part. Subsequently, adding dopamine solution once every ten cycles of CVs, CVs scan was performed continually. The parameters were identical to the first scan until the scan summary reached 30 cycles and then stopped. Thirdly, the counter/reference electrode parts and movable valve were moved away and the washing channels part was folded to overlap with sample pools after electropolymerization. The template CEA entrapped in the MIP membrane were removed thoroughly by 500 μL of SDS/HAC solution (1% HAC and 1 g/L SDS), and then, washed by Milli-Q water to remove excess eluent. As a result, the MIP-ePADs that had specific cavities for CEA was obtained. There are two identical sets of reaction units on the chip. Both units were treated through the same method of synthesizing the MIPs, one of which was served as a blank baseline. The NIP-ePADs was also synthesized under the above conditions without adding CEA templates before electropolymerization.

2.4. Usage of bio-MIP-ePADs

The detailed usage of MIP-ePADs for electrochemical assay procedures was described below. Folding the washing channels part away from the working electrode part, and then, 5 μL human serum samples or different concentrations of CEA solution (10 mM, PBS, pH = 7.4) was added into sample pools, respectively. The chip was left at room temperature for 10 min and then washed 3 times with PBS buffer solution

(10 mM, pH = 7.4). Subsequently, another piece of the counter/reference electrode part (for electrochemical detection) was rotated to overlap with the working electrode part. Finally, 15 μL, 5 mM $[Fe(CN)_6]^{3-/4-}$ (PBS, 0.1 mol/L, pH 7.4) was dropped into the sample pool (electrochemical cell consisting of working electrode part and counter/reference electrode part). Differential pulse voltammetry (DPV) measurements were performed at room temperature in a potential range between −0.2 V and 0.6 V, modulation amplitude of 50 mV, a pulse width of 50 ms and a step potential of 5 mV. Another sample pool could be completed detection by repeating the same procedures.

3. Results and discussion

3.1. Fabrication and operation of bio-MIP-ePADs

There are two sets of same reaction units designed on the chip and every unit contained four functional parts of paper-based chips were designed to fabricate microfluidic paper-based electrochemical device (ePADs) including working electrode part (red colour, 50 mm × 25 mm), two circular pairs counter/reference electrode parts (yellow colour, 24 mm in diameter, one of a pair used for CEA MIP synthesis and another one for CEA detection), movable valve part (blue colour) and washing channels part (green color, 40 mm × 50 mm), respectively(shown in Fig. 1 A, B and Fig. S1A). The Assembly method was shown in Fig. 1 C, D and Fig. S1B, and all the parts are fastened by hollow rivets, except washing channel part. The counter/reference electrode parts and movable valve part can be rotated around the centre of hollow rivets independently. The washing channels part (green colour) and the working electrode part (red colour) could be easily connected by origami folding. Carbon and Ag/AgCl inks were applied on the paper substrates by manual brushing to prepare the carbon and Ag/AgCl electrodes, respectively (as shown in Figs. S1C and D). There were two circular sample pools (9 mm in diameter), a dopamine introducing pool (5 mm in diameter) and two pairs disconnected channels (2 mm width) which can be connected by moveable valve on the working electrode part (Fig. S1D). The paper-based device allowed counter electrode, reference electrode and working electrode to construct two three-electrode systems after rotating counter/reference electrode part to overlap with sample pool (Fig. S1F). The entire assembly process was shown in Supplementary Movie. 1.

The main process of MIP synthesis and Bio-MIP-ePADs application were shown in Fig. 2 and Supplementary Movie. 2. First, all of the counter/reference electrode parts were rotated and separated away from the working electrode part (Fig. 2 A and G). Because the electrical conductivity of the device was one of the important factors for ensuring the sensitivity of the sensing, paper substrate was modified by suitable amount of GO which could improve the conductivity of the paper substrate greatly (Fig. 2 B). Furthermore, graphene oxide has good adsorptive capacity for proteins and biomolecules. Owing this advantage, biomolecular imprinting membranes for electrochemical analysis can be synthesized easily by electropolymerization of dopamine. Chitosan layer on paper-based electrode surface could further improve the adsorption properties (Fig. 2 C). The biological template was difficult to be buried in the caves of the MIPs and form binding site, which was a challenge for electropolymerization of molecular imprinting polymers of bioanalytes. Because the biomolecules had large molecular weights, and a large number of specific groups on the surface of biomolecules were hardly combined with functional monomers. In order to solve this problem, a method of layer-by-layer electropolymerization imprinting was developed in the presence of the bioanalyte on the surface of working electrode. The template molecules were added and adhered to the surface of the paper-based electrode due to the good adsorptive property of cross-linked chitosan (shown in Fig. 2 D). Hereafter, the counter/reference electrode parts (for synthesis) and the movable valve were opened to lead the dopamine solution flowing into sample pool, and then the molecularly imprinted layer was formed by electropolymerization of dopamine (Fig. 2 H). After every 10 cycles of scanning (~10 min), dopamine solution was added by movable valve to keep the electropolymerization continued until the template molecule was well wrapped, and the molecular imprinting was completely formed (Fig. 2 E). The washing channels were opened and eluent was flowed to remove templates (Fig. 2 I). After removal of template molecules (CEA), the CEA-imprinted sites were obtained (Fig. 2 F). The design rotating valves were easy to make flexible operation and let the entire process very convenient and simple. As shown in Fig. 2 J, the incubation lasted for a few minutes after adding the sample. Then sample pool was washing by PBS buffer for removal of excess impurities (Fig. 2 K). When the electrode of ePADs comes into contact with the CEA solution, the CEA was recognized by surface-imprinted layer and then the caves were filled, that blocked the ion transfer pathway. Therefore, the indicator ion cannot enter into the working electrode through the MIPs layer, which resulted in current change (Fig. 2 E and F). Differential pulse voltammetry (DPV) measurements were performed for detecting target in $[Fe(CN)_6]^{3-/4-}$ (Fig. 2 L). The non-imprinted polymer NIP-ePADs was only used as a control because the non-imprinted polymer (NIP) layer was almost completely insulated that no current can be detected.

In this work, synthesis of cancer biomarkers-MIPs layer was firstly introduced into MIP-ePADs by electropolymerization of dopamine (DA) voltammetry (CVs) scanning. The polydopamine layer used to design the imprinted electrochemical sensor has some important desirable advantages: insulation, thinness, and biocompatibility. In addition, dopamine could be an ideal functional monomer for electropolymerization and keep safe and environmentally friendly during the fabrication process. As shown in Fig. S2, there are clear differences between the electropolymerizations process of the MIP and the NIP. It was attributed to the presence of template protein which adsorbed on the surface of the working electrode reducing the conductivity of the ePADs.

3.2. Electrochemical and morphology characterizations

The cyclic voltammetry (CV) responses of bare paper electrode and modified paper electrode were shown in Fig. 3 A. An obvious increase of peak current could be observed when GO was used on bare paper due to the large surface area and high conductivity of GO. Then, a further increase of peak current was obtained after chitosan was coated. It could be attributed to the accelerated electron transfer on the electrode surface because of the electrostatic attraction between positively charged chitosan amino group and negatively charged $[Fe(CN)_6]^{3-/4-}$. The peak current of MIP modified ePADs was very weak before elution, basically as same as that of NIP. After removing templates, the peak current recovered back.

The EIS of different surface modification conditions of the ePADs was shown in Fig. 3 B. The electron-transfer resistance of electrode decrease obviously due to excellent electrical conductivity of graphene oxide. The electron-transfer resistance value further reduced when the chitosan was modified on surface of paper electrode, which verified the cyclic voltammetry characterization results of chitosan of modification. After MIPs and NIPs layer were formed by electropolymerization, the impedance was increased obviously because the protein-embedded molecular imprinting polymer layer blocked electron transfer on surface of electrode. The impedance value was decrease because a large number of cavities were created by removal of the protein templates that ions could go through the polymer to arrive inside of electrode. Finally, the impedance was increased again when the templates protein occurred, which indicated that the template protein was successfully bound to the MIPs. Fig. 3 B (h) and Table S1 is the fitted equivalent circuit diagram, in which R_s, C_{dl}, R_{ct} and Z_w represent the resistance of electrolyte solution, double layer capacitance, chargetransfer resistance and warburg impedance, respectively.

The moveable valve was rotated to open the channel that drive the

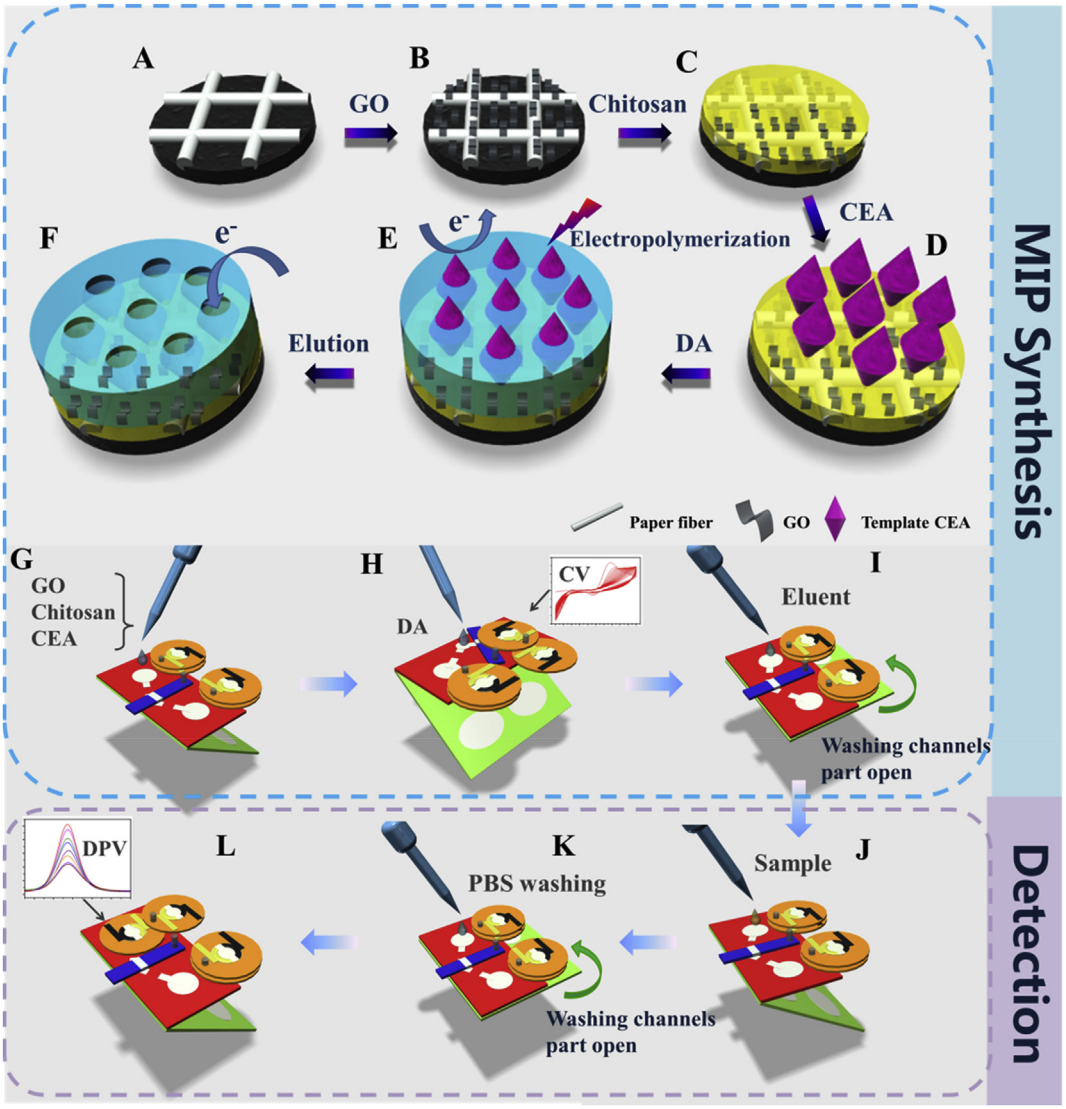

Fig. 2. Figures (A–D) were three-dimensional schematic representation of the fabrication mechanism for this ePADs. (G–L) Schematic diagram of operation process of synthesis CEA molecularly imprinted polymers and detection of CEA by the ePADs. Firstly, GO and chitosan were modified on working electrode pool and CEA template was added (G). (H) Secondly, opening the movable valve and one of the counter/reference electrode parts, the dopamine solution were added in synthetic material pool several times and flowed into the reaction pool by movable valve. The molecularly imprinted polymers were synthetized by electropolymerization. Then, washing channels part was folded to overlap with working electrode pools and the eluent was added to removal of template (I). Thirdly, serum sample was added in working electrode pools (J). Folding washing channels part and washing by PBS buffer solution (K). Opening another counter/reference electrode part, the DPV measurements were performed for detection of CEA (L).

solution from dopamine introducing pool flowing to the sample pool on the working electrode part and the relative reagent was added to the sample pool for carrying out the reaction (Fig. S3). To evaluate the effectiveness of the movable valve in terms of dopamine introducing liquid obviously, two methods (adding liquid was in direct way or through movable valve controlled way) were investigated and the marker in electrochemical cyclic voltammetry was 5 mM $[Fe(CN)_6]^{3-/4-}$. As shown in Fig. 3 C and E, the peak intensity of the cyclic voltammetry curve can be kept stable without significant fluctuations in the next 10 min, after adding PBS buffer solutions (pH 7.4) through the movable valves. This was attributed to the capability of the movable valve which delivered liquid evenly by a smooth diffusion manner. However, as shown in Fig. 3 D and F, the peak intensity of the cyclic voltammetry curve was reduced sharply in a short time, after dropping the PBS buffer solution into the electrode region directly by gravity. Obviously, the manner of direct adding water caused a large degree of uneven concentration of the $[Fe(CN)_6]^{3-/4-}$ on the electrode surface. This confirmed that the relative stability of the distribution of solution diffusion could be promoted and the fluctuation of solution concentration could be reduced on electrode surface.

The surface micro-morphology of working electrode on paper was characterized by scanning electron microscopy (SEM) (Fig. S4). And the plots of anodic peak current versus the square root of scan rates presented linear relationship, suggesting the $[Fe(CN)_6]^{3-/4-}$ redox occurred through a diffusion-controlled electrochemical process (Fig. S5). The SEM images and CVs results indicated that the thickness of PDA layer was appropriate and template molecules could go through the MIPs to arrive at the surface of GO-based working electrode. It also demonstrates that Bio-MIP-ePADs with three electrode system is suitable to perform electrochemical analysis.

3.3. Optimization conditions of the synthesis and detection

The optimized conditions of Bio-MIPs-ePADs were crucial for the sensitive and selective detection of the template. The relative parameters included the amount of template protein, the number of cyclic

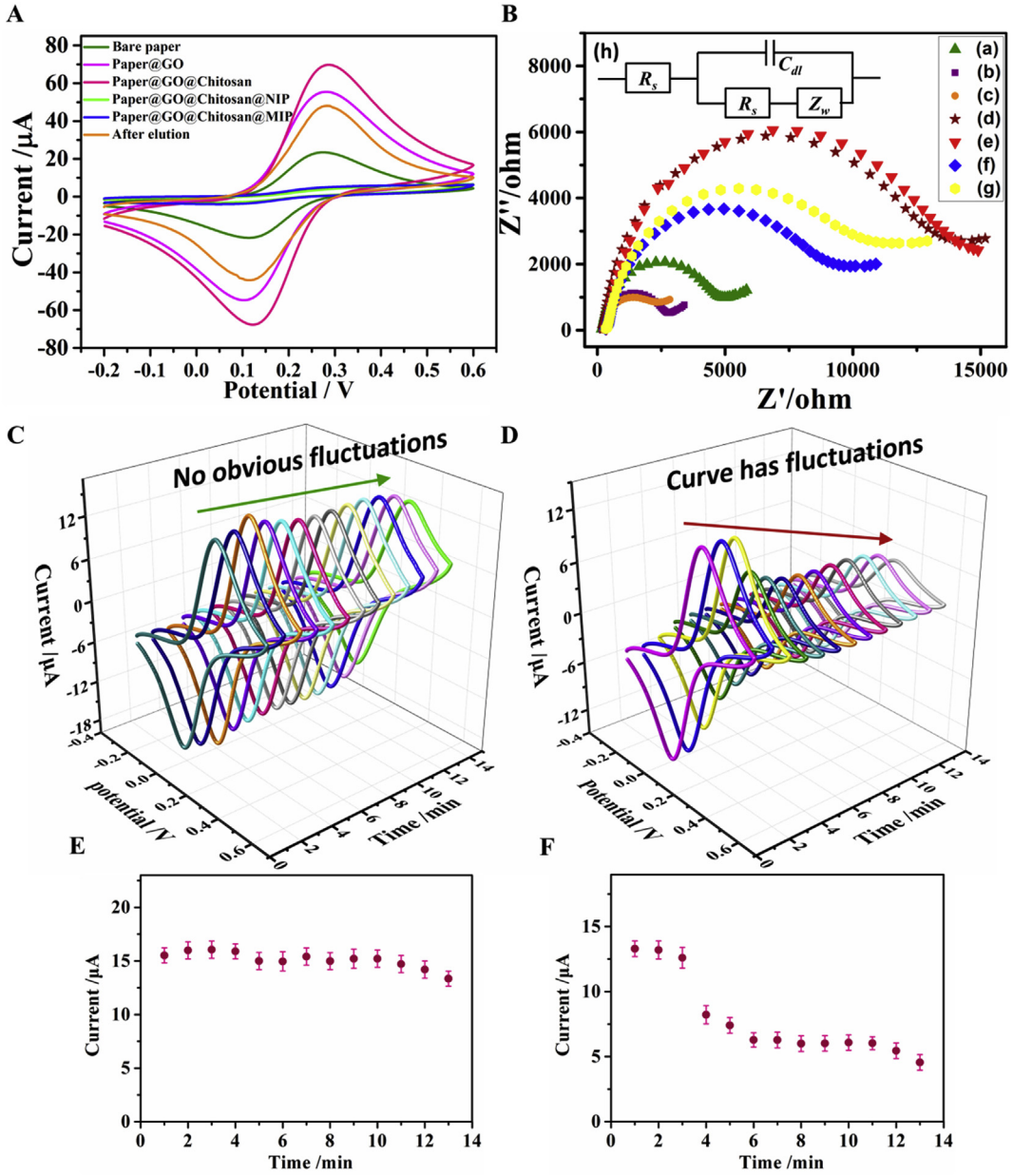

Fig. 3. (A) CVs of the Bio-MIP-ePADs with different surface conditions in 5 mM $[Fe(CN)_6]^{13-/4-}$ (PBS, 0.1 mol/L, pH 7.4). (B) Nyquist diagrams of the Bio-MIP-ePADs under different surface modification in 5 mM $[Fe(CN)_6]^{3-/4-}$ (PBS, 0.1 mol/L, pH 7.4): (a) bare paper electrode; (b) GO modified ePADs; (c) GO and chitosan modified ePADs; (d) MIPs-ePADs before elution; (e) NIP-ePADs; (f) MIPs-ePADs after elution; (g) MIPs-ePADs bind templates again. (h) Equivalent circuit diagram. R_s, C_{dl}, R_{ct} and Z_w represent resistance of electrolyte solution, double layer capacitance, charge-transfer resistance and warburg impedance, respectively. Time dynamic CVs characterization of process of introducing PBS liquid continuously through movable valve (C, No obvious fluctuations) and direct adding by gravity (D, Curve has fluctuations) on the Bio-MIP-ePADs in 5 mM $[Fe(CN)_6]^{3-/4-}$ (PBS, 0.1 mol/L, pH 7.4), and the oxidation peak current value respectively (E and F). The 5 μL PBS buffer solutions were injected 2 min later. (n = 7).

voltammetry scanning of electropolymerization process, elution condition and pH value that were investigated.

It is important to investigate the amount of CEA because the amount of template protein had a great influence on the imprinting effect and selective detection during synthesizing MIPs layer. If the amount of template CEA was few, it would cause that the amount of synthetic cavities were hardly obtained and influence the CV responses of oxidation peak current. In addition, the large amount of template CEA would result in difficulty of forming molecularly imprinted layer and the removal of the template molecules. 5 μL different concentration of template CEA (1, 15, 25, 50, 75, 100, 150, 200 μg/mL CEA) were selected to synthesize MIPs layer for establishing electropolymerization. The current value of CV responses oxidation peak of the Bio-MIPs-ePADs was displayed as the evaluation value (y-axis) after removal of the template CEA. As shown in Fig. 4A, for smaller reagent consumption, 5 μL of 50 μg/mL CEA was chosen in further experiments.

Homogeneous MIPs layer was prepared through the electropolymerization method on the electrode surface. The thickness of the layer was controlled by the number of cyclic voltammetry scanning of electropolymerization process. More importantly, the sensing performance can be considerable affected by the thickness of the surface MIPs layer. We performed cyclic voltammetric characterization for 10, 20, 30 and 40 cycles of electropolymerization process of ePADs (Shown in Fig. 4B). The peak current was almost disappeared after 30 cycles of electropolymerization process that indicated the electrode surface had been completely covered by the imprinted layer. Therefore, considering

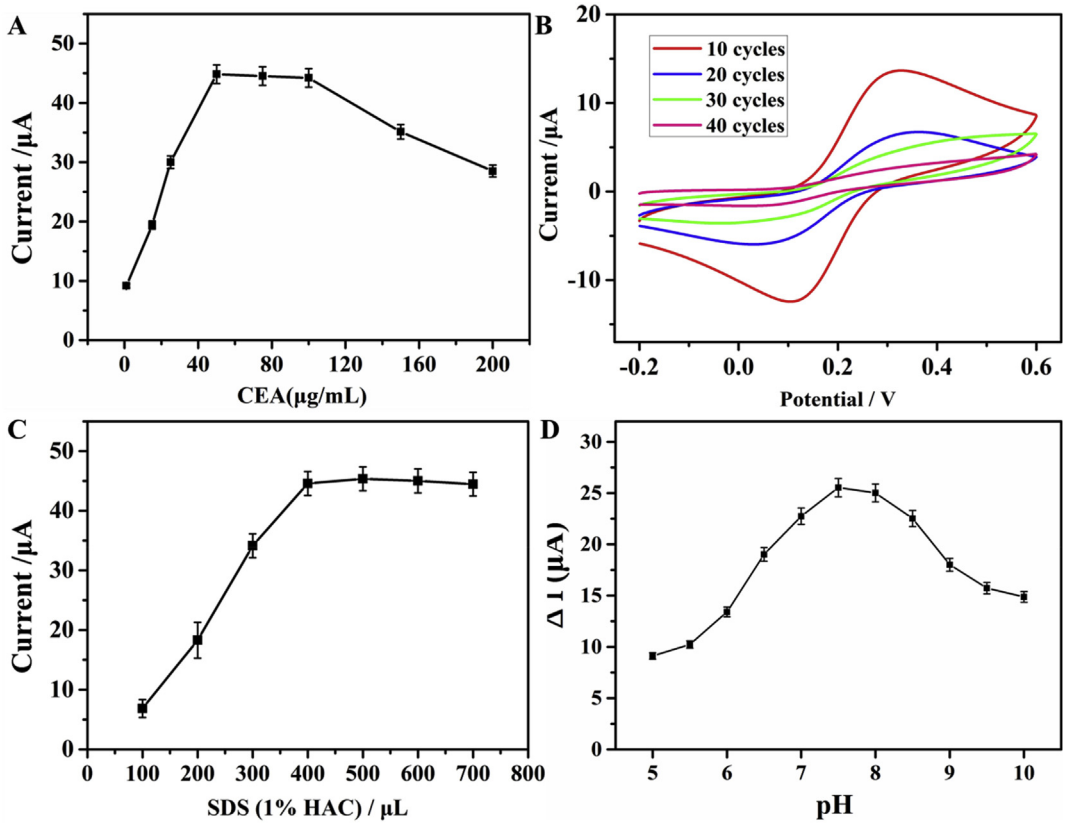

Fig. 4. (A) Influence of the amount of template CEA on the CVs responses oxidation peak current value of the Bio-MIPs-ePADs after elution (eluent were 400 μL). (B) Cyclic voltammetric characterization of electropolymerized dopamine process of Bio-MIPs-ePADs after 10, 20, 30 and 40 cycles. (C) Effect of eluent dosage. (D) Influence of pH on the detection effects of Bio-MIP ePADs (the concentration of CEA was 5 ng/mL, n = 7). All of responses was completed in 5 mM $[Fe(CN)_6]^{3-/4-}$ (PBS, 0.1 mol/L, pH 7.4).

smaller energy and dopamine consumption, 30 cycles of electropolymerization process was chosen in further experiments. In addition, we investigated the effect of scan rates during the process of electropolymerization on sensing performance of Bio-MIP-ePADs (shown in Figs. S6 and S7). Six different scan rates were selected including 10 mV/s, 20 mV/s, 50 mV/s, 80 mV/s, 120 mV/s and 160 mV/s to carry out the process of electropolymerization, respectively. When the scan rate was 20 mV/s, it has displayed good sensing performance of the Bio-MIP-ePADs.

Suitable elution method was critical for the formation of large number of imprinted cavities which could recognize template molecule specifically. The effect of eluting template and the amount of eluent were investigated by detecting the oxidation peak current of $[Fe(CN)_6]^{3-/4-}$ after the synthesis of molecular imprinting. As shown in Fig. 4C, the sample pool of ePADs was eluted by different amounts of eluent after electropolymerization. As the using amount of eluent increased, the template molecules were eluted from the polymer layer and thus the binding cavities were unoccupied and allowed the hexacyanoferrate redox probe to go through them freely. However, excess eluents may damage the strength of the paper fibers. To guarantee the good effect, 500 μL of SDS/HAC solution (1% HAC and 1 g/L SDS) was selected.

The variable parameter for pH was also investigated and shown in Fig. 4D. The effect of DPV peak current reduction value by CEA was poor when pH was less than 7.0 because the solution was too acidic and reduced recognition ability of MIPs. When the pH value increased from 7.0 to 8.0, the peak current reduction value increased greatly, and the peak current reduction value reached its maximum at pH = 7.5. When the pH value was higher than 8.5, the recognition sites on the surface of the imprinted layer were protonated, and the interaction between the molecular imprinting layer binding site and the template was reduced, that leaded to a sharp decrease of peak current reduction value. Taking into account the practical application of the sample analysis, the optimal pH for the Bio-MIPs-ePADs also fitted to the pH range of human serum samples.

To evaluate effect of absorption time of binding sites, dynamic adsorption was investigated over 16 min (the concentration of CEA was 50 ng/mL). The effect of absorption time of Bio-MIP-ePADs had been shown in Fig. S8. It could observe that the absorption reached the equilibrium binding between the MIP and template after 10 min. In order to reduce unnecessary waiting, 10 min of absorption time was chosen in subsequent experiments.

3.4. Analysis performance of bio-MIP-ePADs

The sensitivity and linear range of the sensing performance of Bio-MIP-ePADs were evaluated by the detection of CEA in standard solution at various concentrations. DPV was performed in 5 mM $[Fe(CN)_6]^{3-/4-}$ (PBS, 0.1 mol/L, pH 7.4) with the different concentration of CEA to measure the peak current intensity of the Bio-MIP-ePADs. The DPV peak currents of $[Fe(CN)_6]^{3-/4-}$ decreased with the increasing CEA concentrations on Bio-MIP-ePADs (Fig. 5A). The peak current was proportional to the logarithm value of CEA concentrations in the ranges of 1.0–500.0 ng/mL with the regression equation ΔIp (μA) = 19.342 lgC (ng/mL) + 6.933 and correlation coefficient was 0.994 (Fig. 5B). The detection limit (LOD) was 0.32 ng/mL.

To evaluate the selectivity of the Bio-MIP-ePADs, two different types of potential interference including Bovine Serum Albumin and alpha fetoprotein were detected on Bio-MIP-ePADs. As shown in Fig. 5C, the current responses toward different samples which contain interference had no more obvious responses than sample of CEA. The subtle current response of the interfering species may be due to the fact that the

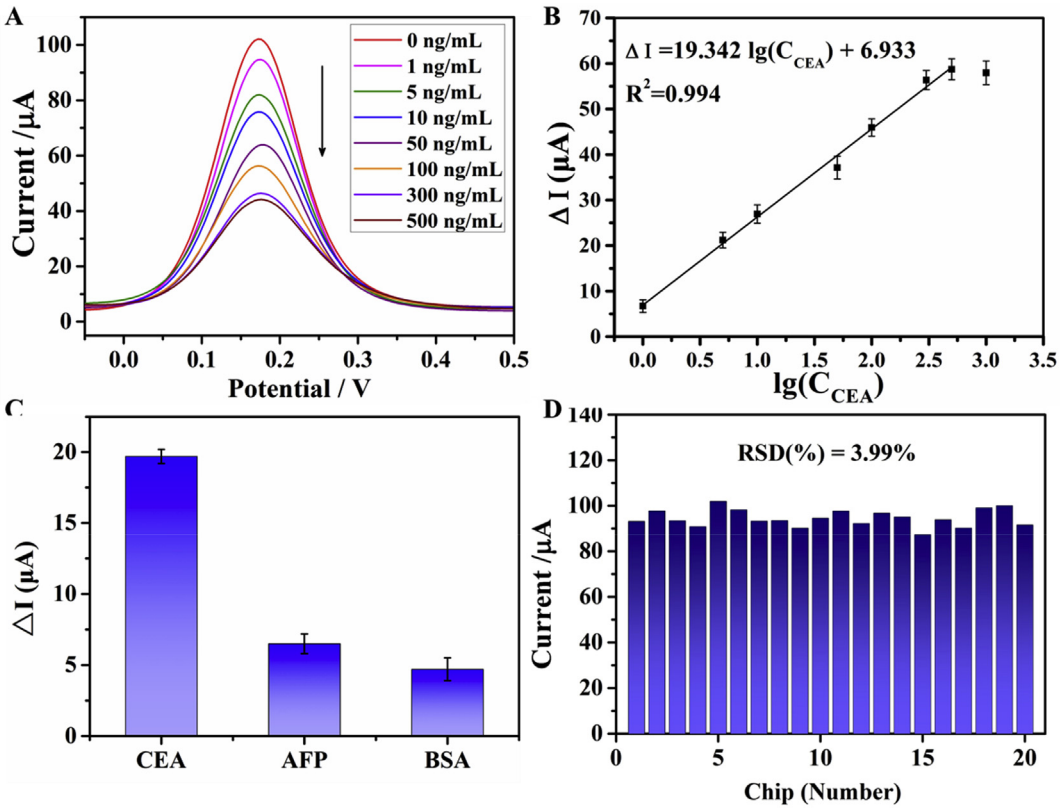

Fig. 5. (A) DPV responses diagrams of Bio-MIPs-ePADs for detection of CEA (CEA concentration was 0, 1, 5, 10, 50, 100, 300, 500 ng/mL respectively). (B) Calibration curves of Bio-MIPs-ePADs for detection of CEA (CEA concentration was 1, 5, 10, 50, 100, 300, 500 1000 ng/mL respectively). (C) Selectivity of Bio-MIPs-ePADs for sample solutions of different interfering targets (Alpha-fetoprotein (AFP) and bovine serum albumin (BSA)). The concentrations of CEA and the interfering targets were 5 ng/mL (n = 5) (D) DPV peaks values of twenty Bio-MIP-ePADs.

polydopamine layer adhered to the insulating protein molecules which caused a certain degree of signal attenuation. The results indicated that the selectivity of the Bio-MIP-ePADs was acceptable. The reproducibility of Bio-MIP-ePADs was evaluated in Fig. 5D and Fig. S9. The relative standard deviation (RSD) of DPV peaks values of twenty Bio-MIP-ePADs was 3.99%. RSD was less than 5% indicating that the chip has good reproducibility. To show the stability of the Bio-MIP-ePADs, we investigated the stability of peak current variation and sensing effect of the device during 18 days at intervals of three days (Fig. S10) to demonstrate good storage stability at room temperature (~25 °C).

To prove the proposed method's performance, a series of CEA standard samples (0.6, 1.2, 2.4, 5.0 ng/mL, respectively) were analyzed in our Bio-MIP-ePADs and, the results was in good agreement with compared ELISA method (As shown in Fig. S11 and Table S2). It indicated the proposed strategy showed good performance and desirable applications. Subsequently, the five real serum samples were analyzed on our Bio-MIPs-ePADs and traditional hospital's chemiluminescent immunoassay (CLIA) method. As shown in Table 1, there were no obvious difference and the RSD of the detection value ranged from 2.7% to 6.5%. It further confirmed that the capability of Bio-MIP-ePADs could provide a feasible alternative tool for the clinical detection in human serum.

Table 1
Assay results of patient serum samples obtained from the proposed Bio-MIP-ePADs and compared with ELISA and hospital chemiluminescent immunoassay (CLIA) methods (n = 3).

Clinical samples	CEA concentration (ng/mL)		
	Proposed method	CLIA	RSD (%)
1	3.53	3.52	2.7
2	1.29	1.14	3.2
3	11.52	12.18	5.4
4	2.95	3.41	5.7
5	1.96	2.15	6.5

4. Conclusions

In summary, a novel paper-based movable valve controlling easy fabrication of dopamine MIP layer and selective and sensitive electrochemical detection of cancer biomarkers on the microfluidic analytical device was presented in this study. This method does not require the use of expensive antibodies, and avoid cumbersome immunoassay steps and antibody storage problems. The whole process is facile and user-friendly. Using dopamine as a functional monomer, a biological molecularly imprinted layer was synthesized on the surface of the paper-based electrode by electropolymerization dopamine method. Carcinoembryonic antigen was applied as model target in our approach and the detection range of CEA was 1.0–500.0 ng/mL, and the detection limit could be achieved as 0.32 ng/mL.

In addition, the method of brushing the surface of the paper fiber is relatively rough. Due to the intricate internal structure of the paper fiber, the working electrical surface is not flat enough, which limits the sensitivity of the device. Future work needs to be improved in the construction of electrodes on paper fibers. In addition, further improvement of the high throughput detection is also the focus for our ongoing work. Briefly, the analysis strategy has the advantages of non-toxicity, low cost, simple operation, high selectivity and high sensitivity, and has shown potential application prospects in the field of clinical diagnosis of POCT.

Conflict of interest

The authors declare no competing financial interest.

Declaration of competing interest

The authors declare that they have no known competing financial interests or personal relationships that could have appeared to influence the work reported in this paper.

CRediT authorship contribution statement

Ji Qi: Conceptualization, Data curation, Formal analysis, Investigation, Methodology, Validation, Writing - original draft, Writing - review & editing. **Bowei Li:** Conceptualization, Investigation, Methodology, Validation, Supervision, Writing - original draft, Writing - review & editing. **Na Zhou:** Methodology. **Xiaoyan Wang:** Methodology. **Dongmei Deng:** Writing - review & editing. **Liqiang Luo:** Investigation, Formal analysis, Project administration, Supervision, Writing - review & editing. **Lingxin Chen:** Conceptualization, Project administration, Methodology, Supervision, Writing - review & editing.

Acknowledgments

This work was financially supported by the National Natural Science Foundation of China (Grant Nos. 41776110, 61571278, 61571280 and 21804010), the National Key Research and Development Program of China (Grant No. 2016YFC1400702), and the Project Sponsored by the Scientific Research Foundation for the Returned Overseas Chinese Scholars, State Education Ministry.

Appendix A. Supplementary data

Supplementary data to this article can be found online at https://doi.org/10.1016/j.bios.2019.111533.

References

Boehle, K.E., Carrell, C.S., Caraway, J., Henry, C.S., 2018. ACS Sens. 3, 1299–1307.
Cai, D., Ren, L., Zhao, H.Z., Xu, C.J., Zhang, L., Yu, Y., Wang, H.Z., Lan, Y.C., Roberts, M.F., Chuang, J.H., Naughton, M.J., Ren, Z.F., Chiles, T.C., 2010. Nat. Nanotechnol. 5, 597–601.
Chen, L., Wang, X., Lu, W., Wu, X., Li, J., 2016. Chem. Soc. Rev. 45, 2137–2211.
Chen, L., Xu, S., Li, J., 2011. Chem. Soc. Rev. 40, 2922–2942.
Chen, S., Chen, X., Zhang, L., Gao, J., Ma, Q., 2017. ACS Appl. Mater. Interfaces 9, 5430–5436.
Cheng, C.M., Martinez, A.W., Gong, J., Mace, C.R., Phillips, S.T., Carrilho, E., Mirica, K.A., Whitesides, G.M., 2010. Angew. Chem. Int. Ed. 49, 4771–4774.
Choleva, T.G., Kappi, F.A., Giokas, D.L., Vlessidis, A.G., 2015. Anal. Chim. Acta 860, 61–69.
Cuartero, M., Crespo, G.A., Bakker, E., 2015. Anal. Chem. 87, 1981–1990.
de Araujo, W.R., Frasson, C.M.R., Ameku, W.A., Silva, J.R., Angnes, L., Paixao, T.R.L.C., 2017. Angew. Chem. Int. Ed. 56, 15113–15117.
Ding, J., Li, B., Chen, L., Qin, W., 2016. Angew. Chem. Int. Ed. 55, 13033–13037.
Dungchai, W., Chailapakul, O., Henry, C.S., 2009. Anal. Chem. 81, 5821–5826.
Economou, A., Kokkinos, C., Prodromidis, M., 2018. Lab Chip 18, 1812–1830.
Ge, L., Wang, S., Yu, J., Li, N., Ge, S., Yan, M., 2013. Adv. Funct. Mater. 23, 3115–3123.
Ge, S., Zhang, L., Zhang, Y., Lan, F., Yan, M., Yu, J., 2017. Nanoscale 9, 4366–4382.
Gervais, L., de Rooij, N., Delamarche, E., 2011. Adv. Mater. 23, H151–H176.
Gong, M.M., Sinton, D., 2017. Chem. Rev. 117, 8447–8480.
Gui, R., Jin, H., Guo, H., Wang, Z., 2018. Biosens. Bioelectron. 100, 56–70.
Han, J., Qi, A., Zhou, J., Wang, G., Li, B., Chen, L., 2018. ACS Sens. 3, 1789–1794.
Haupt, K., Mosbach, K., 2000. Chem. Rev. 100, 2495–2504.
Hu, J., Wang, S., Wang, L., Li, F., Pingguan-Murphy, B., Lu, T.J., Xu, F., 2014. Biosens. Bioelectron. 54, 585–597.
Huang, Y.H., Vakoc, C.R., 2016. Cell 166, 536–537.
Jones, R., 2010. Nature 466, S11–S12.
Kjellgren, H., Gallstedt, M., Engstrom, G., Jarnstrom, L., 2006. Carbohydr. Polym. 65, 453–460.
Kong, Q., Wang, Y., Zhang, L., Xu, C., Yu, J., 2018. Biosens. Bioelectron. 110, 58–64.
Kumar, A.A., Hennek, J.W., Smith, B.S., Kumar, S., Beattie, P., Jain, S., Rolland, J.P., Stossel, T.P., Chunda-Liyoka, C., Whitesides, G.M., 2015. Angew. Chem. Int. Ed. 54, 5835–5852.
Lee, H., Dellatore, S.M., Miller, W.M., Messersmith, P.B., 2007. Science 318, 426–430.
Li, B., Yu, L., Qi, J., Fu, L., Zhang, P., Chen, L., 2017a. Anal. Chem. 89, 5708–5713.
Li, B., Zhang, Z., Qi, J., Zhou, N., Qin, S., Choo, J., Chen, L., 2017b. ACS Sens. 2, 243–250.
Li, W., Yang, H., Chao, M., Li, L., Ge, S., Song, X., Yu, J., Mei, Y., 2014. Electrochim. Acta 141, 391–397.
Liang, R., Ding, J., Gao, S., Qin, W., 2017. Angew. Chem. Int. Ed. 56, 6833–6837.
Liotta, L.A., Ferrari, M., Petricoin, E., 2003. Nature 425 905-905.
Liu, K., Wei, W.Z., Zeng, J.X., Liu, X.Y., Gao, Y.P., 2006. Anal. Bioanal. Chem. 385, 724–729.
Mahadeva, S.K., Walus, K., Stoeber, B., 2015. ACS Appl. Mater. Interfaces 7, 8345–8362.
Manekkathodi, A., Lu, M.Y., Wang, C.W., Chen, L.J., 2010. Adv. Mater. 22, 4059–4063.
Martinez, A.W., Phillips, S.T., Butte, M.J., Whitesides, G.M., 2007. Angew. Chem. Int. Ed. 46, 1318–1320.
Morbioli, G.G., Mazzu-Nascimento, T., Stockton, A.M., Carrilho, E., 2017. Anal. Chim. Acta 970, 1–22.
Nunez-Bajo, E., Carmen Blanco-Lopez, M., Costa-Garcia, A., Teresa Fernandez-Abedul, M., 2018. Talanta 178, 160–165.
Qi, J., Li, B., Wang, X., Fu, L., Luo, L., Chen, L., 2018. Anal. Chem. 90, 11827–11834.
Ruecha, N., Chailapakul, O., Suzuki, K., Citterio, D., 2017a. Anal. Chem. 89, 10608–10616.
Ruecha, N., Lee, J., Chae, H., Cheong, H., Soum, V., Preechakasedkit, P., Chailapakul, O., Tanev, G., Madsen, J., Rodthongkum, N., Kwon, O.-S., Shin, K., 2017b. Int. J. Adv. Manuf. Technol. 2, 1–8.
Sun, X., Li, B., Tian, C., Yu, F., Zhou, N., Zhan, Y., Chen, L., 2018. Anal. Chim. Acta 1007, 33–39.
Wang, P., Sun, G., Ge, L., Ge, S., Yu, J., Yan, M., 2013. Analyst 138, 4802–4811.
Wang, X., Choi, N., Cheng, Z., Ko, J., Chen, L., Choo, J., 2017. Anal. Chem. 89, 1163–1169.
Wulff, G., 2002. Chem. Rev. 102, 1–27.
Xie, C., Li, H., Li, S., Wu, J., Zhang, Z., 2010. Anal. Chem. 82, 241–249.
Yamada, K., Shibata, H., Suzuki, K., Citterio, D., 2017. Lab Chip 17, 1206–1249.
Yang, B., Fu, C., Li, J.P., Xu, G.B., 2018. Trends Anal. Chem. 105, 52–67.
Yang, H., Li, L., Ding, Y.P., Ye, D.X., Wang, Y.Z., Cui, S.G., Liao, L.F., 2017. Biosens. Bioelectron. 92, 748–754.
Yetisen, A.K., Akram, M.S., Lowe, C.R., 2013. Lab Chip 13, 2210–2251.
Zhang, D., Ma, B., Tang, L., Liu, H., 2018. Anal. Chem. 90, 1482–1486.